



## Optimal input design for autonomous aircraft<sup>☆</sup>

G. Licitra<sup>a,b,\*</sup>, A. Bürger<sup>c</sup>, P. Williams<sup>a</sup>, R. Ruitenkamp<sup>a</sup>, M. Diehl<sup>b</sup>

<sup>a</sup> Ampyx Power B.V, The Hague, Netherlands

<sup>b</sup> Department of Microsystems Engineering, University of Freiburg, Germany

<sup>c</sup> Faculty of Management Science and Engineering, Karlsruhe University of Applied Sciences, Germany



### ARTICLE INFO

#### Keywords:

Autonomous aircraft  
Optimum experimental design  
Optimization  
System identification and parameter estimation

### ABSTRACT

Accurate mathematical models of aerodynamic properties play an important role in the aerospace field. In some cases, system parameters of an aircraft can be estimated reliably only via flight tests. In order to obtain meaningful experimental data, the aircraft dynamics need to be excited via suitable maneuvers. In this paper, optimal maneuvers are obtained for an autonomous aircraft by solving a time domain model-based optimum experimental design problem that aims to obtain more accurate parameter estimates while enforcing safety constraints. The optimized inputs are compared with respect to conventional maneuvers widely used in the aerospace field and tested within real experiments.

### 1. Introduction

Nowadays, autonomous aircraft have become widespread for both civil and military applications. An important task for the development of these systems is mathematical modeling of the aircraft dynamics. Such models of aircraft dynamics regularly contain quantities called *aerodynamic derivatives* (or simply *derivatives*), which in general depend on the flight condition and the aircraft geometry.

The current practice is to retrieve derivatives from empirical data obtained from similar aircraft configurations or with tools based on Computational Fluid Dynamics (CFD) and augmenting and verifying them by wind tunnel tests. For standard aircraft configurations such methods are generally in good agreement with experimentally obtained values. However, for less conventional configurations these tools provide only a rough approximation of the aerodynamic properties (Mulder, Van Staveren, & van der Vaart, 2000).

This problem often arises in the Airborne Wind Energy (AWE) community (Diehl, 2013; Fagiano & Milanese, 2012; Fagiano, Nguyen-Van, Rager, Schnez, & Ohler, 2017) where non-conventional high lift aircrafts need to be designed for extremely challenging operational environments (Ruitenkamp & Sieberling, 2013). Fig. 1 shows the CFD analysis of a non-conventional high lift aircraft designed by Ampyx Power B.V. AmpyxPower (2017a). In this case, intensive flight test campaigns must be set in order to gain additional insight about the aerodynamic characteristics.

A successful flight test campaign depends on many factors, such as selection of instrumentation, signal conditioning, flight test operations procedure, parameter estimation algorithm and signal input design. In this paper, the focus is on the optimization of signal inputs that aim to maximize the information content of the measurements data used for determining the aircraft aerodynamic properties via a model-based, time domain approach. A steady reference condition is considered and constraints are enforced in order to prevent flight envelope violation. The optimized experiments are assessed and a real flight test campaign is carried out.

The paper is organized as follows. In Section 2, the mathematical model of the rigid wing aircraft for Optimum Experimental Design (OED) purposes is introduced and a brief overview of the case study designed by Ampyx Power B.V. is provided. Section 3 describes the flight test operation procedure and safety requirements as well as underlying theoretical and practical aspects. Section 4 presents the formulation of the OED problem based on the Cramer–Rao Lower Bound. In Section 5 the performance of the optimized inputs are assessed and compared to the performance of conventional input signals widely used in the aerospace field. The optimal maneuvers are first analyzed via a reliable flight simulator in Section 6 and subsequently experimental data of a real flight test are provided. Section 7 concludes.

<sup>☆</sup> This research was supported by the EU via ERC-HIGHWIND (259 166), ITN-TEMPO (607 957), ITN-AWESCO (642 682), by DFG via Research Unit FOR 2401, and by BMWi via the project eco4wind (0324125B).

\* Corresponding author at: Department of Microsystems Engineering, University of Freiburg, Germany.

E-mail addresses: [giovanni.licitra@imtek.uni-freiburg.de](mailto:giovanni.licitra@imtek.uni-freiburg.de) (G. Licitra), [adrian.buerger@hs-karlsruhe.de](mailto:adrian.buerger@hs-karlsruhe.de) (A. Bürger), [p.williams@ampyxpower.com](mailto:p.williams@ampyxpower.com) (P. Williams), [r.ruitenkamp@ampyxpower.com](mailto:r.ruitenkamp@ampyxpower.com) (R. Ruitenkamp), [moritz.diehl@imtek.uni-freiburg.de](mailto:moritz.diehl@imtek.uni-freiburg.de) (M. Diehl).

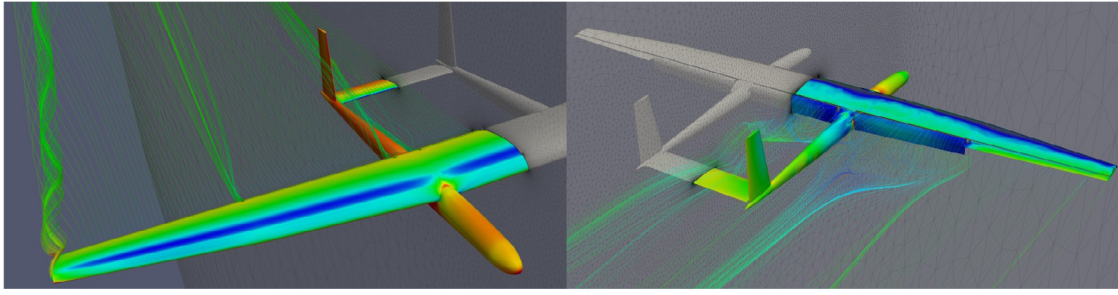


Fig. 1. CFD of the 3rd prototype high lift, rigid wing autonomous aircraft designed by Ampyx Power B.V.

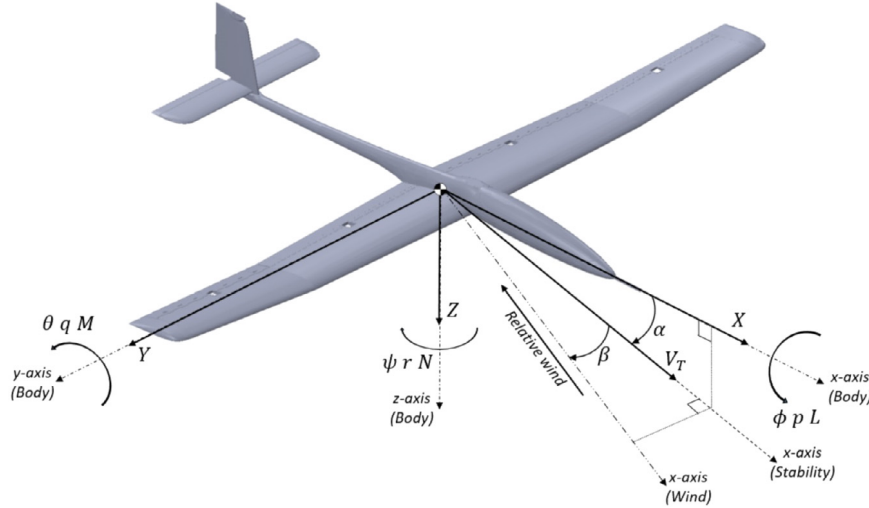


Fig. 2. Definition of axes, Euler angles, aerodynamic states, forces and moments on a rigid wing aircraft.

## 2. Mathematical model

In this section, the mathematical model of a rigid wing aircraft is introduced and a brief overview of the case study is provided.

### 2.1. Modeling of aircraft

For system identification purposes, let us consider the aircraft dynamics as follow (Stevens, Lewis, & Johnson, 2015)

$$\dot{V}_T = \frac{Y \sin \beta + X \cos \alpha \cos \beta + Z \cos \beta \sin \alpha}{m} + G_{V_T}, \quad (1a)$$

$$\dot{\beta} = \frac{Y \cos \beta - X \cos \alpha \sin \beta - Z \sin \alpha \sin \beta}{mV_T} + \frac{G_\beta}{V_T} - r \cos \alpha + p \sin \alpha, \quad (1b)$$

$$\dot{\alpha} = \frac{Z \cos \alpha - X \sin \alpha}{mV_T \cos \beta} + \frac{G_\alpha}{V_T \cos \beta} + \frac{q \cos \beta - (p \cos \alpha + r \sin \alpha) \sin \beta}{\cos \beta}, \quad (1c)$$

$$\dot{\phi} = p + r \cos \phi \tan \theta + q \sin \phi \tan \theta, \quad (1d)$$

$$\dot{\theta} = q \cos \phi - r \sin \phi, \quad (1e)$$

$$\dot{\psi} = \sec \theta (q \sin \phi + r \cos \phi), \quad (1f)$$

$$\dot{p} = \frac{J_{xz}}{J_x} \dot{r} - qr \frac{(J_z - J_y)}{J_x} + qp \frac{J_{xz}}{J_x} + \frac{L}{J_x}, \quad (1g)$$

$$\dot{q} = -pr \frac{J_x - J_z}{J_y} - (p^2 - r^2) \frac{J_{xz}}{J_y} + \frac{M}{J_y}, \quad (1h)$$

$$\dot{r} = \frac{J_{xz}}{J_z} \dot{p} - pq \frac{J_y - J_x}{J_z} - qr \frac{J_{xz}}{J_z} + \frac{N}{J_z}, \quad (1i)$$

where  $(V_T, \beta, \alpha)$  are the aerodynamic states, i.e., true airspeed  $V_T$ , angle of side-slip  $\beta$  and angle of attack  $\alpha$ , whereas the states  $(\phi, \theta, \psi)$  denote the Euler angles of roll, pitch and yaw with  $(p, q, r)$  the corresponding angular body rates (Stevens et al., 2015). The aircraft is assumed to

have a constant mass  $m$ , moments of inertia  $J_x, J_y, J_z$ , cross moment of inertia  $J_{xz}$  and to be subject to external aerodynamic forces  $(X, Y, Z)$ , moments  $(L, M, N)$  and, obviously, gravity. More precisely, the gravity components are expressed as

$$G_{V_T} = g_D (\sin \beta \sin \phi \sin \theta - \cos \alpha \cos \beta \sin \theta + \sin \alpha \cos \beta \cos \phi \cos \theta), \quad (2a)$$

$$G_\beta = g_D (\cos \alpha \sin \beta \sin \theta + \cos \beta \sin \phi \cos \theta - \sin \alpha \sin \beta \cos \phi \cos \theta), \quad (2b)$$

$$G_\alpha = g_D (\sin \alpha \sin \theta + \cos \alpha \cos \phi \cos \theta), \quad (2c)$$

with  $g_D \approx 9.81 \text{ m/s}^2$  the gravitational acceleration. The nomenclature introduced above is summarized in Fig. 2. Furthermore, the mathematical model (1) implicitly presumes that the vehicle is a rigid body with a plane of symmetry such that the moments of inertia  $J_{xy}, J_{xz}$  are zero, whereas the Earth is assumed flat and non-rotating with a constant gravity field (Mulder et al., 2000).

### 2.2. Aerodynamic model

In flight dynamics, there are different methods of aerodynamic derivatives modeling. In many practical cases the aerodynamic forces and moments are approximated by linear terms in their Taylor series expansion. Such approximations yield sufficient accuracy for attached flows at low angles of attack (Etkin, 1972). In this case, the aerodynamic properties can be normalized with respect to the dynamic pressure  $\bar{q} = \frac{1}{2} \rho V_T^2$  with  $\rho \approx 1.225 \text{ kg/m}^3$  the free-stream mass density, and a characteristic area for the aircraft body

$$X = \bar{q} S C_X \quad Y = \bar{q} S C_Y \quad Z = \bar{q} S C_Z \quad (3a)$$

$$L = \bar{q} S b C_l \quad M = \bar{q} S \bar{c} C_m \quad N = \bar{q} S b C_n. \quad (3b)$$

In (3)  $S, b, \bar{c}$  are reference wing area, wing span and mean aerodynamic chord, respectively, while  $C_X, C_Y, C_Z$  denote the forces and  $C_l, C_m, C_n$

Download English Version:

<https://daneshyari.com/en/article/7110236>

Download Persian Version:

<https://daneshyari.com/article/7110236>

[Daneshyari.com](https://daneshyari.com)